

FAST SIMULATION OF REALISTIC SPECT PROJECTIONS USING FORCED DETECTION IN GEANT4

A. Goedicke¹, B. Schweizer¹, S. Staelens², J. De Beenhouwer²

¹Philips Research Laboratories, Weisshausstrasse 2, D-52066 Aachen, Germany

²Ghent University, Elis Department, Sint-Pietersnieuwstraat 41 B-9000 Ghent, Belgium

Email: Andreas.Goedicke@philips.com

Abstract: As in real measurements, the achievable performance of standard Monte-Carlo (MC) based Single Photon Emission Computed Tomography (SPECT) system simulations highly depends on the collimator efficiency. Thus the collimator itself is often excluded from the MC simulation and replaced by an analytical model based on either theoretical (e.g. geometrical) considerations or measurements of the collimator point-spread-function.

If no such theoretical models or measurements are available, the MC approach becomes very time consuming, because most of the simulated particle tracks never reach the detector.

This paper describes the implementation and evaluation of Forced Detection in the widely used MC package GEANT4. It is shown that, using this variance reduction technique, the limitations due to the collimator efficiency can be largely overcome, leading to a highly significant increase in the simulation performance. In an analysis of the results achieved by two different phantom simulation studies, an almost perfect agreement between the standard and the accelerated code with respect to signal intensity, count rate variance and spectral properties is demonstrated. Moreover, different approaches for detector statistics restoration are evaluated. For the given examples, a net performance increase by about a factor of 100 to 160 could be achieved.

Introduction

Monte-Carlo simulations are regarded as the most appropriate methods for SPECT system simulation, since they can emulate any relevant physical effect and can be applied to virtually any system design. A so-called 'analogue' MC simulation, where the number of calculated primary particle histories is equal to the one in a real phantom measurement or patient scan, is especially useful in SPECT system analysis and development since it results in both realistic signal and (quantum) noise properties. However, due to the poor collimator efficiency, an analogue MC simulation is highly inefficient and therefore time consuming. Thus, the collimator itself is often not included in the MC simulation, but its influence on the detector signal is modelled as a kind of post-processing step using convolution kernels based either on theoretical considerations or point-spread-function measurements.

If no such collimator models are available (e.g. if a hypothetical system is simulated) and the collimator influence is also simulated, accurate MC simulations can easily take weeks to months of computation time on modern workstations or small-sized computer clusters.

Numerous so-called 'variance reduction' techniques have been developed in the past in order to overcome this problem and generate highly accurate mean value estimates of stochastic processes with comparatively low numbers of samples. The following section describes the implementation of the so-called Forced Detection (FD) acceleration technique into the widely used MC code package GEANT4 [1]. We will discuss different approaches translating the un-physical statistical properties of the FD detector signal into an image with Poisson statistics. For two different test phantom types, comparisons of the simulated detector count distributions obtained from the conventional analogue MC calculation and from the new FD implementation are presented in section 'Results'. Moreover, figures of the achieved performance improvement are determined from corresponding simulation runs with both methods. In the 'Discussion' section, the results and their consequences for the use of MC simulations in system development are discussed. An outlook on possible further extensions of the implementation concludes the paper.

Materials and Methods

Overview of Variance Reduction Methods: Techniques leading to an efficiency increase over a 'conventional' MC simulation (in the following also termed as 'Brute Force', BF) are called variance reduction methods. These techniques either lead to a reduction in the variance of the MC simulation result for a given number of particle tracks, or alternatively to a reduction of computation time per particle track. The most common variance reduction techniques are known as Sobol' Random Numbers, Woodcock Tracking, Stratification, Importance Sampling, Russian Roulette and Forced Detection; details are found, e.g., in [2]. The technique of Forced Detection (FD) [3][4] is especially suited for the simulation of SPECT cameras since it allows to overcome the geometric inefficiency of the collimator that also limits the efficiency of the BF MC approach.

The Forced Detection Principle: In BF MC simulation, particles are tracked until they are absorbed, their energy drops below a predefined threshold, or they leave the ‘simulation world’. In SPECT, most of these particle tracks do not hit the detector at the end and thus do not contribute to the final detector image. The basic idea of FD is to focus on those tracks with a high probability to pass the collimator and reach the detector. At each interaction point of the BF ‘mother’ photon, a virtual ‘daughter’ photon track is computed, representing the possibility that the interaction makes the mother particle follow a track into the direction of the detector and escape the phantom without any further interaction. Here, ‘into the direction of the detector’ means within a cone around the detector normal that is chosen to be narrow enough to ensure sufficient acceleration of the computation, but wide enough to account for the important physical effects. In the present case, the choice is sufficiently determined by the collimator’s aspect ratio and by the relative fraction of detector counts occurring after penetrating 1, 2, ..., n septa. Within the FD cone, the daughter particle is projected onto the entry plane of the collimator, in order to be tracked from there by a BF MC code again to simulate the collimator including septa penetration or scatter. Finally, in a detector count file each particle is stored with a weight equal to that of the virtual particle used as starting point for the collimator simulation. This principle is schematically illustrated in Figure 1.

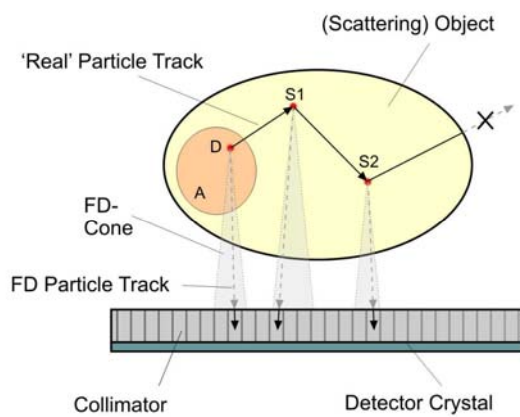


Figure 1: The Forced Detection principle

In order to allow for the directional over-sampling introduced, each particle is assigned a track weight. The daughter particle’s weight is simply computed as the product of the three factors:

- the track probability of the mother before the interaction,
- the probability that the mother particle will be redirected to a path within the pre-defined FD cone, and
- the probability that no further interaction occurs until the particle reaches the collimator surface.

At each interaction site, the mother’s weight, which starts with a value of one, will be reduced by the respective virtual daughter’s weight.

In between interactions, the mother photon will be tracked on as determined by the underlying BF MC code, until it leaves the phantom or is absorbed in it.

Calculating the track weights for the current implementation: The best balance of accuracy and efficiency gain can be obtained with FD by restricting the creation of virtual daughter photons to the most important (mother) photon interaction processes. In the case of a SPECT phantom consisting of soft-tissue equivalent material, these interactions are (a) the nuclear decay itself that creates the mother photons, and (b) Compton scattering. The calculation of the particle weights for these processes is conducted as follows, with the particle type (mother, virtual daughter) denoted as superscript and the creation process labeled using subscripts (decay, compton):

In the case (a) of a nucleus decay event, the probability that a photon (emitted isotropically into 4π sr) propagates towards the detector within the pre-selected emission cone (half opening angle ϑ , solid angle Ω_{Cone}), is equal to $\Omega_{Cone}/4\pi$. Multiplying this directional weight with the probability p_T that the particle reaches the detector without further interaction yields the daughter particle weight:

$$p_d^{(v)} = \frac{\Omega_{Cone}}{4\pi} \cdot p_T = \frac{2}{1 - \cos(\vartheta)} \cdot p_T \quad (1)$$

Accordingly, the weight of the mother particle created in this decay process is:

$$p_d^{(m)} = 1 - p_d^{(v)} \quad (2)$$

When (b) the BF MC algorithm selects a Compton interaction for the mother photon carrying the weight $p_i^{(m)}$ before the interaction, a virtual daughter that propagates towards the detector within the pre-selected cone is created with a weight

$$p_c^{(v)} = p_i^{(m)} \cdot p_T \cdot \sigma_C^{-1} \cdot \int_{\Omega_{Cone}} \left(\frac{d\sigma_C}{d\Omega} \right) d\Omega \quad (3)$$

In this equation, $d\sigma_C/d\Omega$ is the differential Compton cross section per electron. The integral term is normalized to the total Compton cross-section σ_C per electron in order to represent the probability that the mother is scattered into the cone. The mother’s weight after the Compton scattering event is reduced to:

$$p_{i+1}^{(m)} = p_i^{(m)} - p_c^{(v)} \quad (4)$$

From the subsequent collimator and detector BF MC simulation, count weights on the detector are obtained. Summing up the count weights per pixel gives the (downscaled) average count rate in each detector pixel. However, the noise properties of the FD simulation result are not identical to those from the BF simulation. The FD result contains typically a high number of detector counts, each with a small weight, while the true result would contain fewer, integral counts, yielding a higher variance. The increase in detector counts achieved in a FD simulation over that in a BF

simulation with an equal number of mother particles is approximately a factor of $4\pi/\Omega_{Cone}$.

Variance Restoration: The typical procedure for creating realistic noise behaviour in FD simulations is to simulate enough events to achieve a quasi variance-free estimation of the average count rate. This estimate of the mean is then used to generate a new detector signal with appropriate (Poisson) noise properties.

In the present work, an alternative approach for variance restoration is evaluated. Like in the standard FD approach, the calculation of the FD cone probability and transmission probability is performed as described above at each mother event location. But instead of always generating a virtual particle as before, an additional Bernoulli experiment decides whether or not a particle is fed into the BF collimator simulation. A particle with the weight $p^{(v)}_x$ ($x = d, c$) is only allowed to pass on with the probability $p^{(v)}_x/K$, with $K \geq p^{(v)}_{x,max}$. At the same time, the weight of all particles that do pass is set to K . Since it can be shown that a Poisson process followed by a Bernoulli experiment results in a Poisson distribution again, this detector count distribution also includes the correct noise properties. With only isotropic nuclear decay and Compton scatter taken into account as interactions, a good upper estimate K of $p^{(v)}_{x,max}$ is derived by maximising expression (3). In the critical case of a first order ($p^{(m)} \approx 1$) forward Compton event near the object boundary ($p_T \approx 1$), making use of the Klein-Nishina theory [5] yields (with r_e denoting the classical electron radius):

$$K = \sigma_C^{-1} \cdot \Omega_{Cone} \cdot \left. \frac{d\sigma_C}{d\Omega} \right|_{\vartheta=0} = \sigma_C^{-1} \cdot \Omega_{Cone} \cdot r_e^2 \quad (5)$$

For typical SPECT isotope energies, about a fraction $\Omega_{Cone} / (4\pi \cdot K)$ of 30% to 50% of the daughter photons passes the random selection process successfully and is tracked through the collimator. Compared to the BF approach, with the new variance restoration the detector counts for a given number of mother photons are increased by K^{-1} .

These algorithms were implemented into the MC code package GEANT4.

Results

In this section, the FD simulation results are compared to BF GEANT4 simulation results that represent the ‘gold standard’ within the framework of this paper.

Disk Phantom: The first comparison setup features a NEMA sensitivity disk like phantom with a thin layer of Tc-99m solution embedded into a PMMA cylinder with a total thickness of 20 mm and a diameter of 300.0 mm as displayed in Figure 2.

The phantom is located above a pixellated solid state detector, consisting of 167^2 pixels with a pitch of 2.46 mm. Lead absorber plates with one, two and three times a thickness of 0.52 mm, centrally located in the gap between the bottom face of the phantom and the collimator, provide a 140.5 keV-signal attenuation by

about a factor of 4, 16 and 64 in the quadrants Q2, Q3 and Q4 of the detector. In Quadrant Q1 no lead absorber was used, thus the particles remain almost un-attenuated there. The parallel hole lead collimator, with a grid structure matching the detector design, has a height of 45.0 mm and a septal thickness of 0.35 mm and a disk – collimator-distance of 20.0 mm.

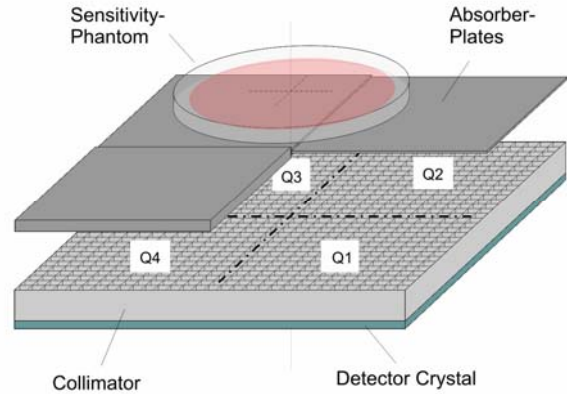


Figure 2: Sensitivity phantom geometry

In the BF GEANT4 simulation, $1.25E10$ primary photons were simulated. In the FD run, only about $4.09E7$ mother photons had to be simulated for a chosen FD cone angle of $\vartheta = 4.42^\circ$ according to the calculated count rate increase of 304.5. For easier and more accurate comparison of the simulation results, a perfect detector energy resolution and Detector Quantum Efficiency (DQE) was assumed. Figure 3 shows the spectra achieved from the BF run and the FD approach with the Bernoulli statistics restoration.

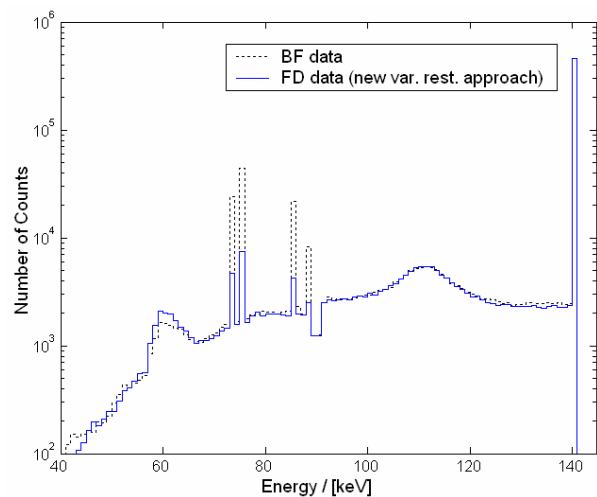


Figure 3: Spectra from the disk phantom simulation

Although both spectral plots are generally in good agreement, it can be seen from the spectra that due to the chosen FD cone angle the lead fluorescence is quantitatively underestimated by the FD approach, since the out-of-cone areas of the collimator, which also contribute to that part of the spectrum, are not hit by virtual particles. Thus this effect reflects an inherent

limitation of the acceleration method. If an accurate modelling of the lead fluorescence is required, either the FD cone has to be enlarged accordingly, which diminishes the simulation performance, or additional corrections have to be applied. We therefore restrict the further quantitative and statistical analysis of the simulation results to counts with energies above 90 keV.

Figure 4 shows the results of a variance analysis separately performed for each of the quadrants on the detector. For each of these sectors, the plot displays the relative difference between the measured variance in the number of counts per detector pixel and the expected variance calculated as the square root of the measured mean number of detector counts per pixel. Moreover, four different simulation approaches are compared: BF as ‘gold standard’, FD with the new variance restoration method, standard FD without Poisson noise restoration and conventional Poisson restoration created from standard FD after pre-filtering the detector image with a 3x3-Median-filter). To prevent segment boundary gradients, only data from center areas are analysed. Each sector dataset still contains 1719 (pixel) samples.

All the approaches with variance restoration are in good agreement with the BF results. The FD results without variance restoration are also included and demonstrate the non-Poissonian nature of the non-corrected FD detector.

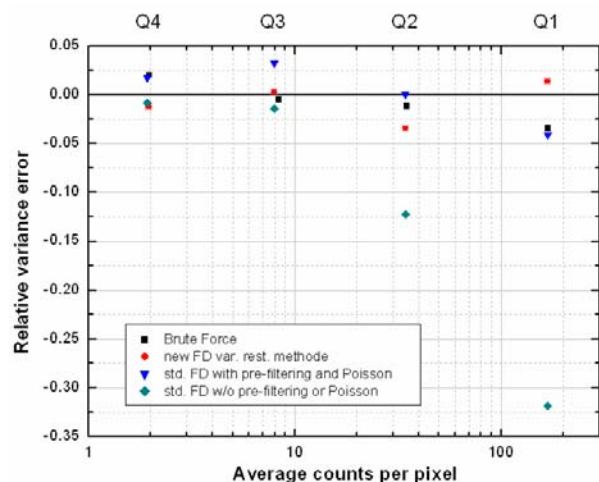


Figure 4: Variance analysis for different methods

Cylindric scattering phantoms: The next phantom geometry consists of a 200.0 mm Tc-99m line source with negligible thickness embedded in a PMMA cylinder with a height of 240.0 mm and with diameters of 10 cm, 20 cm and 30 cm, as schematically shown in Figure 5. Even though the activity distribution is not realistic for clinical cases, the geometry of the scattering cylinder roughly approximates the diameter range in SPECT patient anatomy from a child’s head to the abdomen of an adult. The cylinder was tilted at an angle of 5.0° with respect to the collimator grid in order to reduce grid artefacts in the detector image. The detector/collimator chosen is in principle identical to that used in the sensitivity phantom simulation. Only the number of detector elements (and the number of

collimator cells) has been increased to 179² pixels with a pitch of 2.46 mm each.

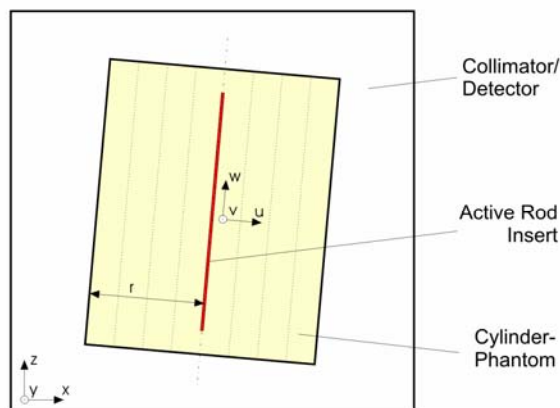


Figure 5: Line phantom with scattering cylinders of different size.

The number of particles simulated for each BF and FD run are identical to those of the former simulation. The distribution of detector counts along a direction perpendicular to the cylinder axis is displayed in Figure 6. It clearly demonstrates that the FD method used agrees qualitatively and quantitatively with the BF simulation and is well suited to create a good description of the underlying scatter background in SPECT images within a short simulation time.

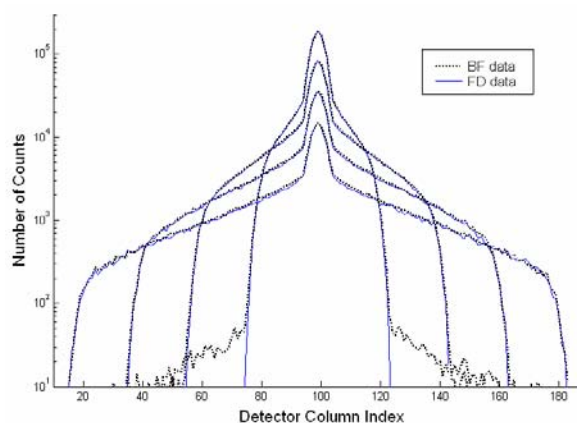


Figure 6: Detector count distribution accumulated along w-axis and displayed along u-axis for different PMMA cylinder diameters

The slight scatter background underestimation in the FD data visible both at the edge of the smallest cylinder as well as next to the central peak is attributed to the omission of the modelling of Rayleigh scattering in the current FD implementation. This is clearly demonstrated by the perfect match of both curves in Figure 7, where the same analysis was performed under exclusion of all detected particles which have undergone one or more Rayleigh events in their track history.

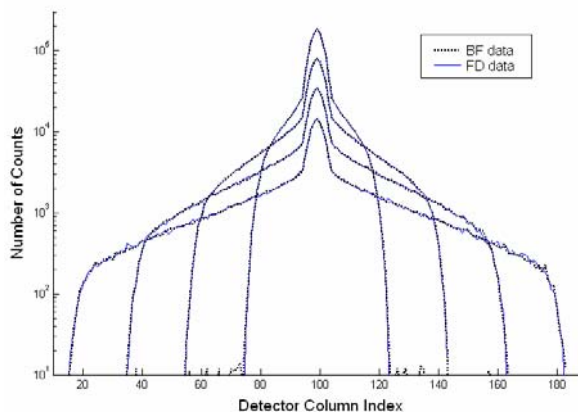


Figure 7: Cylinder phantom simulation results, but Rayleigh scattered particles excluded from analysis.

Acceleration: In the preceding section, a factor of K^{-1} was derived for the increase of detector counts per given number of mother particles compared to a BF simulation. A true acceleration measurement should also include the additional computational effort for the virtual daughter particles. Therefore, simulation runs with both the FD and the BF method with an equivalent number of decay events were run on the same computer (Dell Precision Workstation 670, 2 x Intel Xeon CPUs, 2.8GHz, 1Gbyte RAM, OS: Linux Red Hat Enterprise WS rel. 3). Table 1 gives the ratios of BF to FD simulation time, representing the true acceleration factor gained by our FD approach over a BF MC simulation.

Simulation	$\vartheta / [^\circ]$	K^{-1}	$\frac{t_{sim}^{(BF)}}{t_{sim}^{(FD)}}$
Disk Phantom	4.42	304.5	159
Cylinder Phantom (CP): r = 50 mm r = 100 mm r = 150 mm r = 200 mm	4.42	304.5	105
	4.42	304.5	110
	4.42	304.5	113
	4.42	304.5	115
Antrop. Chest Phantom	3.8	391.6	149

Table 1: Achieved detector countrate increase and simulation speed-up for various phantom setups

Anthropomorphic Chest Phantom: An exemplary projection of a SPECT study using a pixellated solid-state (CZT) detector and calculated with the accelerated simulation engine is shown in Fig. 8. In this dual isotope study, a voxelized static cardiac phantom (including body, spine, lungs, mediastinum, myocardium and liver volumes) was imaged in 64 projections on a 168 x 168 detector matrix with a total number of about 1E7 detector events. The collimator has a height of 45.0 mm with a pixel pitch of 2.46 mm. The complete simulation

run took about 4 days on a compute cluster with 20 (dual-processor) nodes. Even taking into account the additional computational effort introduced with the FD method, the observed simulation speed-up was 149 compared to a standard GEANT4 run.

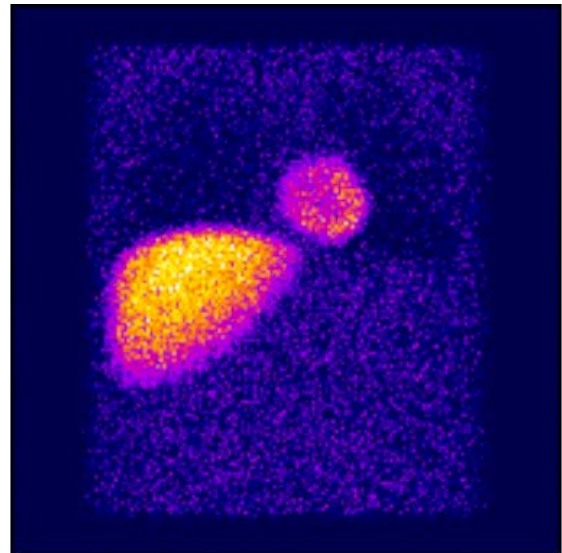


Figure 8: Simulation of an anthropomorphic chest phantom scan.

Discussion

The strategy for accelerating SPECT image simulations presented in this paper consists of the implementation of the FD principle in GEANT4 and an additional stochastic process that converts the weighted virtual counts into a distribution of integer counts at the top level of the collimator. It has been demonstrated in comparative simulation runs between the FD and the BF codes that the calculation results are in very good agreement with respect to spectral, intensity and noise properties and the physical expectations. The acceleration achieved with the implementation from this paper over a BF GEANT4 run is on the order of 105 to 159.

Given the possibility to simulate realistic SPECT projections within hours or days at detector count numbers similar to those from a real patient measurement, as compared to weeks or even months of simulation time with a BF approach, MC simulations can be used for a much wider range of tasks for SPECT system analysis, optimisation and design. One example for a study that has become possible only by the development of this acceleration approach is the theoretical investigation of the performance of SPECT reconstruction algorithms under varying data acquisition parameters. In these studies, a full set of typically 64-128 projections has to be simulated. The noise properties of these projections need to be absolutely realistic since they strongly affect the reconstruction result.

It should be noted that the FD implementation of this work currently only covers the effects of nuclear decay

and Compton scattering. While this is sufficient for most situations, an extension of the FD routines to Rayleigh scattering or photoelectric effect might be needed in some cases. Especially lead detector fluorescence is not dealt with in exactly the same manner as in the BF approach. The narrow emission cone selected for the virtual daughters is wide enough to contain all directions that have a significant probability of leading to a detector count, either by direct passage of the collimator hole or by single or dual septal penetration. In contrast to this, a BF approach also simulates many photons impinging under inclined directions onto the collimator septa, which will practically never yield a direct count, but possibly create lead K-fluorescence photons with energies between about 73 keV and 88 keV that can hit the detector. Therefore, the BF simulation yields a broad lead fluorescence count distribution on the detector that is not created at full intensity in the current implementation of FD. In most situations, signals below approximately 100 keV are never recorded or used in a SPECT procedure, but if the collimator fluorescence is of interest for the analysis (e.g. in SPECT studies using Tl-201 or I-125), additions to the code should be made.

Conclusions and Outlook

This paper describes the acceleration of SPECT projection simulations in MC by using a combination of FD and stochastic particle sampling. With the reduction in calculation time by more than two orders of magnitude, MC simulation at realistic countrates was turned into a practical development and design tool for SPECT systems and procedures.

Further extensions of the simulation system will include modelling of collimator fluorescence, especially for obtaining a good background estimate also in the energy window of SPECT isotopes with photon energies below 100 keV as well as the development of a dedicated Rayleigh-FD routine.

Acknowledgements

We would like to thank our colleagues Heinrich v. Busch, Herfried Wiczorek, Rolf Bippus and Henrik Botterweck for stimulating discussions and valuable contributions. The UGent-coauthors were supported by the Institute for the Promotion of Innovation by Science and Technology in Flanders (IWT, Belgium), and by the Ghent University.

References

- [1] AGOSTINELLI S. *et al.* (2003): 'GEANT4 – A Simulation Toolkit', *Nucl. Instr. and Methods in Physics Research Section A: Accelerators, Spectrometers, Detectors and Associated Equipment*, 506, Issue 3, pp. 250-303
- [2] KAWARAKOW I. and FIPPEL M. (1999): 'Investigation of variance reduction techniques for Monte Carlo photon dose calculation using XVMC', *Phys. Med. Biol.*, 45, pp. 2163-2183
- [3] BECK J. W. *et al.* (1982): 'Analysis of SPECT including scatter and attenuation using sophisticated Monte Carlo modelling methods', *IEEE Trans. Nucl. Sci.*, NS-29, 1, pp. 506-511
- [4] HAYNOR R. D., HARRISON L., LEWELLEN K. (1991): 'The use of importance sampling techniques to improve the efficiency of photon tracking in emission tomography simulations', *Med. Phys.*, 18, 5, pp. 990-1001
- [5] LEO W. R. (1994): 'Techniques for Nuclear and Particle Physics Experiments', 2nd rev. edition, Springer-Verlag Berlin